

# ON THE MINIMUM CORE MASS FOR GIANT PLANET FORMATION THROUGH KELVIN-HELMHOLTZ CONTRACTION

ANA-MARIA A. PISO  
 Harvard-Smithsonian Center for Astrophysics

ANDREW N. YODIN  
 JILA, University of Colorado at Boulder  
*Draft version February 13, 2013*

## ABSTRACT

The core accretion model proposes that giant planets form by the accretion of gas onto a solid protoplanetary core. Previous studies have found that there exists a “critical core mass” past which hydrostatic solutions can no longer be found and unstable atmosphere collapse occurs. In standard calculations of the critical core mass, planetesimal accretion deposits enough heat to alter the luminosity of the atmosphere, increasing the core mass required for the atmosphere to collapse. In this study we consider the extreme case in which planetesimal accretion is negligible and Kelvin-Helmholtz contraction dominates the luminosity evolution of the planet. We develop a two-layer atmosphere model with an inner convective region and an outer radiative zone that matches onto the protoplanetary disk, and we determine the minimum core mass for a giant planet to form within the typical disk life timescale for a variety of disk conditions, which we denote as “critical core mass”. We find that the absolute minimum core mass required to nucleate atmosphere collapse within the disk lifetime is smaller for planets forming further away from their host stars. Moreover, the critical core mass is strongly dependent on disk temperature, opacity and mean molecular weight of the gas. Our results yield lower mass cores than corresponding studies for large planetesimal accretion rates. We therefore show that it is easier to form a planet by growing the core first, then accreting a massive gaseous envelope, rather than forming the core and atmosphere simultaneously.

## 1. INTRODUCTION (PAPER II)

Current theories of giant planet formation postulate that these planets form either through core accretion (refs), in which solid planetesimals collide and grow into a massive solid core, which then accretes a gaseous envelope, or due to a gravitational instability in the protoplanetary disk that leads to fragmentation of the disk into self-gravitating clumps (refs, inc. D’Angelo et al. 2011).

Standard core accretion models (refs) assume that the core and the atmosphere grow at the same time, and that planetesimal accretion deposits enough heat to alter the luminosity of the atmosphere, increasing the core mass required for the atmosphere to collapse, while the heat generated by the gravitational (Kelvin-Helmholtz) contraction of the atmosphere is neglected. These studies consider that the planet atmosphere is in steady state, in which all the luminosity due to planetesimal accretion is radiated away by the envelope, and find that there exists a minimum (“critical”) core mass past which hydrostatic solutions can no longer be found and unstable atmosphere collapse occurs.

Forming giant planets at wide separations in the disk poses theoretical challenges. On the one hand, gravitational instability generates objects that are too massive to explain the current observed properties of exoplanets (refs, inc. Rafikov 2005). On the other hand, planetesimal accretion is slow at large distances in the disk, and therefore large cores may not be able to form before the dissipation of the disk (refs). I would therefore be easier if giant planets could form from smaller cores which

would need less time to grow.

In this study, we show that giant planets can grow faster from small protoplanetary cores that are fully formed before significant gas accretion occurs. In this scenario, the planetesimal accretion rate is significantly slowed down during the gas contraction phase of the atmosphere. This reduction can arise due to dynamical clearing, or due to the core having formed in the inner parts of the disk and migrated outwards, etc. In this situation, the atmosphere evolution is dominated by the Kelvin-Helmholtz contraction of the envelope. The atmosphere is no longer in a steady state, but rather it accretes gas as it loses energy through radiation.

In our model we therefore assume that the luminosity evolution of the atmosphere is dominated by gas contraction, while the planetesimal accretion rate is negligible. As a result, the protoplanetary core has a fixed mass. We consider that the atmosphere evolves in time through stages of quasi-static equilibrium. Once the mass of the gaseous envelope becomes comparable to the mass of the solid core, the self-gravity of the atmosphere can no longer balance the pressure gradient and unstable hydrodynamic collapse commences. The time required for the atmosphere to grow to this stage is the characteristic growth time of the atmosphere. For a set of fixed gas and disk conditions, there exists a minimum core mass for which the atmosphere can grow on the time scale described above within the life time of the protoplanetary disk, which we define as the “critical core mass”.

We develop a two-layer atmosphere model, with a convective inner region and a radiative outer region that

matches smoothly on to the protoplanetary disk, and develop a cooling model that evolves the atmosphere in time. We aim to find the critical core mass for a giant planet to form before the dissipation of the disk.

This paper is organized as follows. In section 2 we describe the assumptions of our atmosphere model, and derive the basic equations that govern the structure and evolution of the atmosphere. In section 3, we present a simplified analytic model that predicts the qualitative behavior of the numerical model. We describe our results in section 4, and determined the critical core mass for planet formation during the life time of the protoplanetary disk in section 5. We discuss our results in section 6 and summarize our findings in section 7.

## 2. ATMOSPHERE MODELS (PAPER I)

In this section we derive the structure and evolution of a planetary atmosphere embedded in a protoplanetary disk in the absence of planetesimal accretion. In section 2.1 we describe the assumptions of our model. In section 2.2 we describe the properties of our assumed protoplanetary disk and review relevant length scales. Section 2.3 presents the equations describing the structure of a static planetary atmosphere and the boundary conditions that we use. In section 2.4 we develop a model to estimate the rate at which the atmosphere cools. Finally, we combine these calculations into a quasi-static model for atmospheric evolution in section 2.5.

### 2.1. Basic Model Assumptions

We develop a two-layer atmosphere model with the following assumptions:

1. The planet consists of a solid core of fixed mass and a two-layer atmosphere composed of an inner convective zone and an outer radiative zone that matches smoothly on to the disk, as mentioned in section. The two regions are separated by the Schwarzschild criterion for convective instability (see section 2.3). We denote the surface between the two regions as the radiative-convective boundary (RCB), which is henceforth defined by a radius  $r = R_{RCB}$ .
2. The luminosity evolution of the atmosphere is dominated by Kelvin-Helmholtz contraction rather than planetesimal accretion.
3. The luminosity is assumed to be constant throughout the outer radiative region. Since the structure of the convective zone is independent of its luminosity, we do not need to make additional assumptions about the luminosity in this region.
4. The envelope evolves through stages of quasi-static equilibrium.

We use assumptions for the atmosphere geometry and composition similar to those of previous studies (e.g., Ikoma et al. 2000, Papaloizou & Nelson 2005), as follows:

1. The atmosphere is self-gravitating, spherically symmetric and in hydrostatic balance.

2. The atmosphere consists of a hydrogen-helium mixture, with hydrogen and helium mass fractions of 0.7 and 0.3, respectively.

The time dependence of the atmosphere structure equations may be neglected or explicitly taken into account. Some previous studies of atmosphere accretion (e.g., Stevenson 1982, Wuchterl 1993, Rafikov 2006) consider static envelopes, in which the luminosity is solely supplied by planetesimal accretion and fully radiated away by the atmosphere. In other studies, the time evolution is explicitly taken into account and full time dependent models are developed (e.g., Ikoma et al. 2000). We follow an intermediate approach and consider quasi-static evolution. Our model for the atmosphere growth time is described in section 2.4.

### 2.2. Disk Model and Length Scales

As a disk model, we use the minimum mass, passively irradiated model of Chiang & Youdin (2010). In this model, the surface density and mid-plane temperature are given by

$$\Sigma_d = 2200 F_\Sigma a^{-3/2} \text{ g cm}^{-2} \quad (1a)$$

$$T_d = 120 F_T a^{-3/7} \text{ K}, \quad (1b)$$

with  $a$  the semi-major axis in AU, and  $F_\Sigma$  and  $F_T$  normalization factors that adjust the disk mass and temperature relative to the minimum mass solar nebula (MMSN). In this study, we assume  $F_\Sigma = F_T = 1$ . The resulting mid-plane pressure is given by

$$P_d = 1.1 \times 10^{-4} F_\Sigma \sqrt{F_T m_*} a^{-45/14} \text{ dyne cm}^{-2} \quad (2)$$

for a molecular weight  $\mu = 2.35$ . Here  $m_* \equiv M_*/M_\odot$ , where  $M_*$  is the mass of the central star and  $M_\odot$  is the mass of the Sun. We take  $m_* = 1$ .

We further define several characteristic length scales that are important for this problem.

**The Core Radius** represents the physical radius of the protoplanetary core:

$$R_c \equiv \left( \frac{3M_c}{4\pi\rho_c} \right)^{1/3}, \quad (3)$$

with  $M_c$  and  $\rho_c$  the core mass and density, respectively. Since we assume that the core mass does not change with time, the core radius is also fixed for a given model.

**The Bondi Radius** represents the distance from the planet at which the thermal energy of the nebular gas is of the order of the gravitational energy binding the gas to the planet. It is defined as

$$R_B \equiv \frac{GM_p}{c_s^2} = \frac{GM_p}{\mathcal{R}T_d}, \quad (4)$$

where  $G$  is the gravitational constant,  $M_p$  is the total mass of the planet,  $c_s$  is the sound speed, and  $\mathcal{R}$  is the reduced gas constant:  $\mathcal{R} = k_b/(\mu m_p)$ , with  $k_b$  the Boltzmann constant and  $m_p$  the proton mass.

**The Hill Radius** represents the distance at which the gravitational attraction of the planet and of the host star are comparable. It is given by

$$R_H \equiv a \left( \frac{M_p}{M_\odot} \right)^{1/3} \quad (5)$$

Outside the Hill radius, the gravity of the core is too weak to affect the nebular gas. Consequently, the planet will be able to accrete only gas that lies within its Hill sphere.

**The Disk Scale Height** is defined by

$$H \equiv \frac{c_s^2}{\Omega}, \quad (6)$$

where  $\Omega$  is the Keplerian angular velocity. The disk scale height is a measure of the thickness of the protoplanetary disk. Using equation (1a), we find that the scale height for our assumed disk model can be expressed as

$$H = 0.022 \sqrt{F_T} a^{9/7} \text{ AU} \quad (7)$$

For small planet masses,  $R_B < R_H < H$ . As the atmosphere becomes more massive, tidal truncation becomes more important than thermal constraints, and  $R_H < R_B < H$ . Finally, for high mass atmospheres the disk scale height becomes smaller than the Hill radius of the planet, and spherical symmetry breaks, as the planet is now affected by the vertical profile of the disk.

### 2.3. Structure Equations and Boundary Conditions

An atmosphere in hydrostatic equilibrium is fully described by the following structure equations:

$$\frac{dP}{dr} = -\frac{Gm}{r^2} \rho \quad (8a)$$

$$\frac{dm}{dr} = 4\pi r^2 \rho \quad (8b)$$

$$\frac{dT}{dr} = \nabla \frac{T}{P} \frac{dP}{dr} \quad (8c)$$

$$\frac{dL}{dr} = 4\pi r^2 \rho \epsilon_g, \quad (8d)$$

where  $r$  is the radial coordinate,  $P$ ,  $T$  and  $\rho$  are the gas pressure, temperature and density, respectively,  $m$  is the mass enclosed by the radius  $r$ ,  $L$  is the luminosity from the surface of radius  $r$ , and  $\epsilon_g \equiv -T \frac{ds}{dt}$  represents the heating per unit mass due to gravitational contraction, with  $s$  the specific gas entropy. The temperature gradient  $\nabla \equiv \frac{d \ln T}{d \ln P}$  has different expressions depending on the primary means of energy transport throughout the atmosphere. We assume that energy can be transported either through radiation or convection. When the luminosity is carried by radiative diffusion, the temperature gradient is given by

$$\nabla = \nabla_{\text{rad}} \equiv \frac{3\kappa P}{64\pi G m \sigma T^4} L, \quad (9)$$

where  $\sigma$  is the Stefan-Boltzmann constant and  $\kappa$  is the opacity. Alternatively, when the energy is transported

outwards through convective motions, the temperature gradient becomes

$$\nabla = \nabla_{\text{ad}} \equiv \left( \frac{d \ln T}{d \ln P} \right)_{\text{ad}}, \quad (10)$$

where  $\nabla_{\text{ad}}$  is the adiabatic temperature gradient. For an ideal gas of adiabatic index  $\gamma$ ,  $\nabla_{\text{ad}} = \frac{\gamma-1}{\gamma}$ . The process that dominates energy transport throughout the atmosphere is determined by the Schwarzschild criterion (e.g., Thompson 2006): the atmosphere is stable against convection when

$$\nabla < \nabla_{\text{ad}} \quad (11)$$

and convectively unstable when the reverse is true. In order for convection to be effective,  $\nabla \approx \nabla_{\text{ad}}$ . Therefore, we find that the temperature gradient is given by  $\nabla = \min(\nabla_{\text{ad}}, \nabla_{\text{rad}})$ .

In order for equation set (8) to be solvable, it has to be supplemented by an equation of state (EOS) that relates pressure, temperature and density  $P = P(\rho, T)$ , and an opacity law for  $\kappa$ . In our study, we assume an ideal gas polytropic EOS

$$P = K \rho^\gamma = K \rho^{1/(1-\nabla_{\text{ad}})}, \quad (12)$$

with  $K$  the adiabatic constant. The adiabatic gradient is  $\nabla_{\text{ad}} = 2/5$  for a monatomic gas and  $\nabla_{\text{ad}} = 2/7$  for a diatomic gas. Additionally, the ideal gas law relates the pressure, temperature and density through

$$P = \rho \mathcal{R} T, \quad (13)$$

with  $\mathcal{R}$  defined in section 2.1. The specific gas constant  $\mathcal{R}$  depends on the mean molecular weight of the gas  $\mu$ .  $\mu$  is determined by the relative abundance of hydrogen and helium in the atmosphere. In this study we assume that the helium fraction only affects the molecular weight of the gas, and not the adiabatic index. We show in section 5.3 that this assumption does not affect the qualitative behavior of our solutions.

We assume an opacity power law of the form

$$\kappa = \kappa_0 \left( \frac{P}{P_d} \right)^\alpha \left( \frac{T}{T_d} \right)^\beta, \quad (14)$$

with  $\alpha$  and  $\beta$  constants, and  $\kappa_0 = 2F_\kappa$ . To estimate  $\alpha$  and  $\beta$  we use the Bell & Lin (1994) opacity laws for ice grains:  $\alpha = 0$ ,  $\beta = 2$  and  $F_\kappa = 1$  (i.e.,  $\kappa_0 = 2$ ). We note that these values are valid only for low disk temperatures:  $T_d < \sim 100\text{K}$ . As such, we only consider cool atmospheres that form in the outer part of the protoplanetary disk ( $a \geq 10 \text{ AU}$ ).

#### 2.3.1. Boundary Conditions

We assume a solid core of fixed mass  $M_c$  with a radius given by equation (3). We choose  $\rho_c = 3.2 \text{ g cm}^{-3}$  (e.g., Papaloizou & Terquem 1999). Furthermore, we assume the atmosphere extends out to the boundary of the Hill sphere, defined by equation (5). If the Bondi radius (defined in equation (4)) is within the Hill radius, perturbations of the nebular gas still occur past the Bondi radius due to the gravitational influence of the core. If,

on the other hand,  $R_B > R_H$ , then the Hill radius is the more relevant truncation radius since material cannot be gravitationally bound to the protoplanet outside the Hill sphere. As such, it is always safe to choose the Hill radius as the outer boundary.

As stated in section 2.1, the atmosphere matches smoothly onto the disk at the outer boundary. The temperature and pressure at the Hill radius have to therefore be given by the nebular temperature and pressure:  $T(R_H) = T_d$  and  $P(R_H) = P_d$ .

#### 2.4. Virial Equilibrium and Global Cooling Model

Section 2.3 provides the structure model for a static atmosphere. We now derive the time evolution of the atmosphere due to Kelvin-Helmholtz contraction between subsequent static models.

We first describe the general ways in which planetary Kelvin-Helmholtz contraction differs from the stellar case.

An isolated sphere, such as a star, satisfies a simple global energy equation:

$$L = \Gamma - \dot{E}, \quad (15)$$

where the total luminosity  $L$  is balanced by the rate of heat generation  $\Gamma$  (due to nuclear fusion in the case of star) and the rate at which total energy is lost  $\dot{E}$ . The total energy of the sphere is given by the sum of the gravitational and internal energies.

A protoplanetary atmosphere that is not isolated, but is embedded in a gas disk, satisfies a more complex cooling equation:

$$L = L_c + \Gamma - \dot{E} + e_{\text{acc}}\dot{M} - P_M \frac{\partial V_M}{\partial t} \quad (16)$$

This cooling model applies at any radius  $R$  where the mass enclosed is  $M$ , for example the Bondi radius or the Hill radius.  $L$ ,  $\Gamma$  and  $\dot{E}$  are the same as in equation (15), and include the atmosphere from the core to the top boundary. The gravitational energy  $E_G$  of an atmosphere with total mass  $M$  is given by

$$E_G = - \int_{M_c}^M \frac{Gm}{r} dm, \quad (17)$$

while the internal energy is

$$U = \int_{M_c}^M u dm, \quad (18)$$

where  $u$  is the internal energy per mass. We now explain the additional terms in the cooling equation (16).  $L_c$  is the luminosity from the solid core, and may include planetesimal accretion and radioactive decay.  $e_{\text{acc}}$  is the specific total energy brought in by mass accreting at the rate  $\dot{M}$ :  $e_{\text{acc}} = u - GM/R$ . The last term represents the work done on a surface mass element.

The global cooling equation can be derived starting from the local cooling balance. Integrating the local energy equation and (8d) from the core to the surface and using equation (8b) yields

$$L - L_c = \int_{M_c}^M \frac{\partial L}{\partial m} dm \quad (19a)$$

$$= \int_{M_c}^M \left( \epsilon - T \frac{\partial s}{\partial t} \right) dm \quad (19b)$$

$$= \Gamma - \int_{M_c}^M \frac{\partial u}{\partial t} dm + \int_{M_c}^M \frac{P}{\rho^2} \frac{\partial \rho}{\partial t} dm, \quad (19c)$$

where  $\Gamma = \int_{M_c}^M \epsilon dm$  and equation (19c) follows from equation (19b) through the first law of thermodynamics.

Moreover, a self-gravitating protoplanetary atmosphere has to satisfy virial equilibrium. The virial theorem is derived by integrating the equation of hydrostatic balance (8a) and has the form

$$E_G = -3 \int_{M_c}^M \frac{P}{\rho} dm + 4\pi(R^3 P_M - R_c^3 P_c) \quad (20)$$

Similarly to the cooling equation, it applies at any radius  $R$  where the total mass enclosed is  $M$ . For an ideal gas of adiabatic index  $\gamma$ , equation (20) leads to the following expression for the total energy:

$$E = (1 - \xi)U + 4\pi(R^3 P_M - R_c^3 P_c) \quad (21a)$$

$$= \frac{\xi - 1}{\xi} E_G + \frac{4\pi}{\xi} (R^3 P_M - R_c^3 P_c) \quad (21b)$$

The global cooling equation (16) can therefore be derived using equations (19) and (20). A detailed derivation is deferred to Appendix A.

#### 2.5. Quasi-Static Two-Layer Model

As a consequence of the equations derived in section 2.4, both the atmosphere structure and the gas accretion rate are uniquely determined by the current atmosphere mass. As this mass accretion rate is slow compared to the time it takes to relax to this solution, we can make a quasi-static model of the atmosphere growth. In this section we therefore describe the procedure to obtain an evolutionary series from the cooling model introduced in 2.4 between consecutive two-layer static atmospheres (cf. 2.1).

We use the boundary conditions and opacity laws described in section 2.3. The numerical integration is performed through the shooting method, which solves the boundary value problem by reducing it to an initial value problem: trial values are chosen for the parameters at one of the boundaries, then the equations are integrated and the resulting values at the other boundary are compared to the actual boundary conditions. The procedure is repeated until convergence is achieved. We start with a total atmosphere mass  $M_i$ , where the index  $i$  labels each evolutionary stage. For this mass we guess a trial luminosity  $L = L_{\text{guess}}$ . The assumption of constant luminosity throughout the radiative zone sets the right hand side of equation (8b) to zero, i.e. the time dependence is neglected. We integrate the structure equations (8) inwards from  $R_{\text{out}} = R_H$ , with the boundary conditions

$T(R_{\text{out}}) = T_d$  and  $P(R_{\text{out}}) = P_d$ . The numerical integration gives a value for the core mass implied by the trial solution  $M_c = M_{c,\text{guess}}$ . We adjust  $L_{\text{guess}}$  until  $M_{c,\text{guess}}$  converges to the actual core mass  $M_c$ .

The time evolution of the atmosphere is obtained using the global cooling model described in section 2.4. We neglect the luminosity due to planetesimal accretion and direct heat generation; as such, the first two terms in equation (16) are set to zero. Equation (16) is then evaluated at the RCB, since we assume that luminosity is primarily generated in the convective zone. In what follows,  $X_{RCB}$  denotes quantity  $X$  evaluated at the RCB. The time step  $\Delta t_i$  between two consecutive models of masses  $M_i$  and  $M_{i+1}$  is calculated as follows:

$$\begin{aligned} \langle L \rangle_i \Delta t_i = & -\Delta E_{RCB,i} + \langle e_{\text{acc},RCB} \rangle_i \Delta M_{RCB,i} \\ & - \langle P_{RCB} \rangle_i \Delta V_{RCB,M,i} \end{aligned} \quad (22)$$

where we denote

$$\Delta X_i = X_{i+1} - X_i \quad (23a)$$

$$\langle X \rangle_i = \frac{X_i + X_{i+1}}{2} \quad (23b)$$

The subscript  $M$  in the volume expression above signifies evaluating the change in volume at constant mass.

By connecting sets of subsequent static atmospheres through the procedure described above we therefore obtain an evolutionary atmosphere series.

### 3. ANALYTIC COOLING MODEL (PAPER I)

In this section we derive a simplified analytic model for the atmosphere structure and evolution, based on the assumptions and equations described in section 2. We use this model to predict the qualitative behavior of our more detailed numerical model.

We consider a two-layer atmosphere structure model as presented in section 2.1. We approximate the outer radiative zone of the atmosphere as nearly isothermal. Moreover, we do not take into account the self-gravity of the atmosphere in either region. In the next subsections we derive the structure and cooling behavior of such an atmosphere, deferring some of the calculations to Appendix B.

#### 3.1. Isothermal Atmosphere

We now consider the structure of a low mass (non self-gravitating) isothermal atmosphere. We assume the atmosphere matches onto a constant background density,  $\rho_o$ , at a distance  $r_{\text{fit}} = n_{\text{fit}} R_B$ . The resulting density profile is

$$\rho = \rho_d \exp\left(\frac{R_B}{r} - \frac{1}{n_B}\right) \approx \rho_d \exp\left(\frac{R_B}{r}\right), \quad (24)$$

where the approximate inequality holds deep inside the atmosphere ( $r \ll R_B$ ) for any  $n_{\text{fit}} \gtrsim 1$ . However the choice of boundary condition does have an order unity effect on the density near the Bondi radius. In our study,  $n_{\text{fit}} = R_B/R_H$ , when the Bondi radius is larger than the Hill radius, and  $n_{\text{fit}} = 1$  when the opposite is true.

The mass of the atmosphere is typically determined by integrating the density profile from the core to the

Bondi radius. Planets can attract massive atmospheres if  $\theta_c \equiv R_B/R_c \gg 1$ . In this case

$$M_{\text{iso}} \approx 4\pi\rho_o \frac{R_c^4}{R_B} e^{R_B/R_c} = 4\pi\rho_o \frac{R_c^3}{\theta_c} e^{\theta_c}. \quad (25)$$

This result is the leading order term in a series expansion. Furthermore, because the atmospheric scale-height at  $R_c$  is  $H_\rho = |dr/d\ln\rho| = R_c^2/R_B$ , the result is intuitively the correct order of magnitude.

#### 3.2. Temperature and Pressure Corrections at the Radiative-Convective Boundary

We now show that the temperature contrast between the radiative-convective boundary  $T_{RCB}$  and the ambient disk  $T_d$ , is modest. From equation (9), we express the radiative lapse rate

$$\nabla_{\text{rad}} = \frac{3\kappa P}{64\pi GM\sigma T^4} L = \nabla_o \frac{(P/P_d)^{1+\alpha}}{(T/T_d)^{4-\beta}} \quad (26)$$

where the second equality follows from the opacity law (14), and  $\nabla_o$  is the radiative temperature gradient at the disk:

$$\nabla_o \equiv \frac{3\kappa_0 P_d}{64\pi GM\sigma T_d^4}. \quad (27)$$

$M$  is the sum of the core mass and the atmosphere mass below the pressure level  $P$ . If the mass in the radiative zone is small, then we can hold  $M$  fixed at the sum of the core and convective zone masses:  $M = M_c + M_{\text{conv}}$ . With this assumption and power-law opacity, we get a constant value for  $\nabla_o$ . The temperature profile then integrates to

$$\left(\frac{T}{T_d}\right)^{4-\beta} - 1 = \frac{\nabla_o}{\nabla_\infty} \left[ \left(\frac{P}{P_d}\right)^{1-\alpha} - 1 \right], \quad (28)$$

where  $\nabla_\infty = (1+\alpha)/(4-\beta)$  is  $\nabla_{\text{rad}}$  for  $T, P \rightarrow \infty$ .<sup>1</sup> We apply Equations (26) and (28) at the radiative-convective boundary (where  $\nabla_{\text{rad}} = \nabla_{\text{ad}}$ ) under the assumption that the pressure there is  $P_{RCB} \gg P_d$ , motivated by the fact that the exponential density and hence pressure profile is isothermal (see equation (24)). The resulting temperature contrast at the radiative-convective boundary is

$$\chi \equiv \frac{T_{RCB}}{T_d} \simeq \left(1 - \frac{\nabla_{\text{ad}}}{\nabla_\infty}\right)^{-\frac{1}{4-\beta}}. \quad (29)$$

For  $\alpha = 0$  and  $\beta = 2$ , and assuming  $\nabla_{\text{ad}} = 2/7$ , we find  $\chi \approx 1.5$ . Values of  $\chi$  and  $\nabla_\infty$  for other choices of  $\beta$  are summarized in Appendix B.

The pressure at the convective boundary follows from Equations (9) and (29) as

$$\frac{P_{RCB}}{P_d} \simeq \left(\frac{\nabla_{\text{ad}}/\nabla_o}{1 - \nabla_{\text{ad}}/\nabla_\infty}\right)^{\frac{1}{1+\alpha}} \quad (30)$$

This pressure contrast can be quite large due to the smallness of  $\nabla_o$  in low luminosity atmospheres.

<sup>1</sup> Our definitions of  $\nabla_o$  and  $\nabla_\infty$  are precisely opposite to Rafikov (2006), but consistent with other works and the general convention of labeling a quantity  $f$  in the disk as  $f_o$ .

It is also useful to obtain a relation between  $T$  and  $P$  that eliminates  $\nabla_o$  in favor of  $P_{\text{RCB}}$ :

$$\frac{T}{T_d} = \left\{ 1 + \frac{1}{\frac{\nabla_\infty}{\nabla_{\text{ad}}} - 1} \left[ \left( \frac{P}{P_{\text{RCB}}} \right)^{1-\alpha} - \left( \frac{P_d}{P_{\text{RCB}}} \right)^{1-\alpha} \right] \right\}^{\frac{1}{4-\beta}}. \quad (31)$$

We can determine the radius of the convective boundary  $R_{\text{RCB}}$  from the hydrostatic balance equation as

$$\frac{R_B}{R_{\text{RCB}}} = \int_{P_o}^{P_{\text{RCB}}} \frac{T}{T_d} \frac{dP}{P}. \quad (32)$$

An isothermal atmosphere gives a simple logarithmic dependence on  $P_{\text{RCB}}$ . However using Equation (31) in the integral gives

$$\frac{R_B}{r_{\text{RCB}}} = \ln \left( \frac{P_{\text{RCB}}}{P_o} \right) - \ln \theta, \quad (33)$$

with an extra correction term,  $\theta < 1$ . The form we chose for the correction term allows us to relate the disk and radiative-convective boundary pressures as :

$$P_{\text{RCB}} = \theta P_d e^{R_B/R_{\text{RCB}}}. \quad (34)$$

In the  $P_{\text{RCB}} \gg P_d$  limit the correction term is an order unity constant that depends on  $\alpha$ ,  $\beta$  and  $\nabla_{\text{ad}}$ . Similarly to the temperature correction factor  $\chi$ ,  $\theta$  accounts for the fact that the radiative region is not perfectly isothermal. For  $\nabla_{\text{ad}} = 2/7$ , we find  $\theta(\alpha = 0, \beta = 20) \approx 0.556$ . Values of  $\theta$  for other choices of  $\beta$  are summarized in Appendix B. A simple analytic expression for  $\theta$  is not possible.

### 3.3. Simplified cooling model

We now use a simplified version of the cooling model introduced in section 2.4 in order to obtain an analytic cooling model. As before, we assume a polytropic equation of state and neglect self-gravity.

#### 3.3.1. Luminosity, Energy & Mass

From equation (26), the luminosity that emerges at the radiative-convective boundary is

$$L_{\text{RCB}} = \frac{64\pi G M_{\text{RCB}} \sigma T_{\text{RCB}}^4 \nabla_{\text{ad}}}{3\kappa P_{\text{RCB}}} \approx L_o \frac{P_d}{P_{\text{RCB}}}, \quad (35)$$

where we drop the pressure dependence from the opacity law (14) and

$$L_o \equiv \frac{64\pi G M_{\text{RCB}} \sigma T_d^4 \nabla_{\text{ad}} \chi^{4-\beta}}{3\kappa(T_d) P_d} \quad (36)$$

normalized to disk conditions, with  $T = \chi T_d$  at the RCB.

For  $\beta = 2$  and  $F_\kappa = 1$  in the opacity law (14), this gives the Bell & Lin (1994) opacity for icy grains. By varying  $F_\kappa$ , dust depletion or enhancement can be considered. Grain properties affect both  $F_\kappa$  and  $\beta$  which generally satisfies  $1/2 \lesssim \beta \lesssim 2$  (aside from discontinuities across sublimation regions, see Semenov et al. (2003)).

To make further analytic progress, we ignore the self-gravity in the convective zone, holding the mass fixed at  $M_c$ . The density profile of an adiabatic atmosphere follows from hydrostatic balance as

$$\rho = \rho_{\text{RCB}} \left[ 1 + \frac{R'_B}{r} - \frac{R'_B}{R_{\text{RCB}}} \right]^{1/(\gamma-1)}. \quad (37)$$

where we define an effective Bondi radius,

$$R'_B \equiv \frac{G M_c}{C_P T_{\text{RCB}}} = \frac{\nabla_{\text{ad}}}{\chi} R_B \quad (38)$$

to simplify expressions.

Deep in the atmosphere, where  $r \ll R_{\text{RCB}} \lesssim R'_B$  the density profile is  $\rho \propto r^{-1/(\gamma-1)}$ . Since the energy scales as  $\rho r^2 \propto r^{(2\gamma-3)/(\gamma-1)}$  only polytropes with  $\gamma < 3/2$  (i.e.  $\gamma = 7/5$ , but not  $\gamma = 5/3$ ) have the bulk of energy at the bottom of the atmospheres. We will thus focus on the  $\gamma = 7/5$  case, even though dissociation occurs deep in real protoplanetary atmospheres.

The total (thermal and gravitational) energy in an adiabatic atmosphere could be evaluated from the virial theorem (see section 2.4). More simply, we use the result for temperature profiles in deep (but non-self-gravitating) convective regions:

$$T \approx \frac{G M_c}{C_P r} = T_{\text{RCB}} \frac{R'_B}{r}. \quad (39)$$

The internal energy per unit mass of an ideal gas is thus  $u = C_V T = (1 - \nabla_{\text{ad}}) G M_c / r$  and the specific energy deep in the atmosphere is

$$e = e_g + u = -\nabla_{\text{ad}} \frac{G M_c}{r}. \quad (40)$$

Thus the total energy for  $\gamma < 3/2$  is thus

$$E = -4\pi \nabla_{\text{ad}} G M_c \int_{R_c}^{R_{\text{RCB}}} \rho r dr \quad (41)$$

$$\approx -4\pi P_{\text{RCB}} R'_B \frac{1}{\nabla_{\text{ad}}} \left( \frac{\gamma-1}{3-2\gamma} \right) R_c^{\frac{2\gamma-3}{\gamma-1}} \quad (42)$$

$$\approx -8\pi P_{\text{RCB}} \frac{R_B'^{7/2}}{\sqrt{R_c}} \quad (43)$$

where the final expression takes  $\gamma = 7/5$ .

The mass of the adiabatic atmosphere is given by

$$M_{\text{atm}} = 4\pi \int_{R_c}^{R_{\text{RCB}}} \rho r^2 dr \quad (44)$$

$$= \frac{5\pi^2}{4} \rho_{\text{RCB}} R_B'^{5/2} \sqrt{R_{\text{RCB}}} \quad (45)$$

in the limit  $R_c \ll R_{\text{RCB}} \ll R'_B$ . The mass in the isothermal region is  $M_{\text{iso}} \sim 4\pi \rho_{\text{RCB}} r_{\text{RCB}}^4 / R_B \ll M_{\text{atm}}$ , and can be neglected.

We can eliminate  $R_{\text{RCB}}$  using Equation (34). The ratio of atmosphere to core mass is then

$$\frac{M_{\text{atm}}}{M_c} \approx \frac{P_{\text{RCB}}/P_M}{\sqrt{\ln[P_{\text{RCB}}/(\theta P_d)]}} \quad (46)$$

where we introduce a characteristic pressure

$$P_M \equiv \frac{4\nabla_{\text{ad}}^{3/2}}{5\pi^2 \sqrt{\chi}} \frac{G M_c^2}{R_B'^4}. \quad (47)$$

For the atmosphere to initiate unstable gas accretion,  $M_{\text{atm}} = M_c$ . We thus require

$$P_{\text{RCB}} = \xi P_M \quad (48)$$

where the logarithmic factor

$$\xi \equiv \sqrt{\ln[P_{\text{RCB}}/(\theta P_d)]} = \sqrt{\ln[\xi P_M/(\theta P_d)]} \quad (49)$$

is found by numerically solving the above transcendental equation. The physical solution has  $\xi > 1$ , but typically order unity. Numerical solutions exist for  $\xi \ll 1$ , but are unphysical as they imply  $P_{\text{RCB}} < P_d$ .

### 3.3.2. Cooling Time

Neglecting the surface terms from equation (16), the total time to cool the atmosphere from an initially fully adiabatic state is <sup>2</sup>

$$t_{\text{cool}} = - \int \frac{dE}{L} = - \int_{P_o}^{P_{\text{RCB}}} \frac{dE/dP_{\text{RCB}}}{L} dP_{\text{RCB}} \quad (50)$$

$$\approx 4\pi \frac{P_{\text{RCB}}^2}{P_o} \frac{R_B'^{7/2}}{L_o \sqrt{R_c}}, \quad (51)$$

where we neglect self-gravity and take  $M_{\text{RCB}} = M_c$  in  $L_o$ .

The cooling timescale for an atmosphere to become self-gravitating is found from Equations (51) and (48) as

$$t_{\text{cool}} \approx 2 \times 10^8 \frac{F_T^{5/2} F_\kappa \left(\frac{\xi}{3.4}\right)^2}{\left(\frac{m_{c\oplus}}{10}\right)^{5/3} \left(\frac{a}{10}\right)^{15/14}} \text{ yr} \quad (52)$$

for  $\beta = 2$  and  $m_{c\oplus} \equiv M_c/M_\oplus$ . Clearly this timescale is too long, and this is likely due to missing physics of self-gravity and EOS. Nevertheless the trends are informative. A reduction in opacity naturally gives faster cooling, as long as the optically thick assumption holds. Lower disk temperatures also give faster cooling. Even though higher temperatures give higher luminosities, they also give higher dust opacities and lower the Bondi radius and gas density. On the other hand, higher temperatures suppress cooling in this model. For different  $\beta$  values, the temperature dependence is  $t_{\text{cool}} \propto F_T^{\beta+1/2}$ . The cooling timescale only weakly depends on disk mass or pressure, via the logarithmic factor  $\xi$ . This weak dependence is a consequence of cooling coming from the radiative-convective boundary. Note that the scaling laws do not reflect the changes to  $\xi$  which remains order unity.

### 3.3.3. Critical Core Mass

We can define a critical more mass as that which gives a self-gravitating atmosphere within a typical gas disk lifetime:

$$t_{\text{cool}} = 3 \times 10^6 \tau_{\text{cool}} \text{ yr}, \quad (53)$$

with  $\tau_{\text{cool}}$  a scaling factor. The resulting critical core mass is

$$M_{\text{crit}} \approx 100 \frac{F_T^{3/2} F_\kappa^{3/5} \left(\frac{\xi}{2.6}\right)^{6/5}}{\left(\frac{a_\oplus}{10}\right)^{9/14}} M_\oplus. \quad (54)$$

As with the cooling time, the critical mass is too large due to missing physics. The scaling with disk properties

<sup>2</sup> The relevance of the neglected surface terms is discussed in Appendix B

is similar, in fact all quantities are simply raised to the 3/5 power. The  $\xi$  value is changed to match the value for the nominal solution. The lower value reflects the fact that an atmosphere around such a massive core does not need to contract as much to be self-gravitating.

The numerical values for a different opacity law do not change the numerical answers above very much. That is mostly because we have chosen a disk location where  $T_d$  is not far from 100 K, where our opacity law is normalized. More generally a higher  $\beta$  value is more favorable for core accretion at large distances due to the sharper drop in opacity. The effects of opacity on the cooling time and critical core mass are discussed in appendix Appendix B

## 4. QUASI-STATIC KELVIN-HELMHOLTZ CONTRACTION (PAPER I)

In this section we describe our choices for the gas, disk and core parameters, and present some typical atmosphere numerical models. As mentioned in section 2.1, we assume that the central star is a Sun-like star with  $M_* = M_\odot$ . We are primarily interested in the outer regions of the protoplanetary disk, so we generate atmosphere models between 10 and 100 AU. As a fiducial case, we assume that the atmosphere is composed of a hydrogen-helium mixture with the helium mass fraction  $Y = 0.3$ , resulting in a mean molecular weight  $\mu = 2.35$ . We do not take into account the dependence of the adiabatic index on the helium fraction, and therefore assume the adiabatic index for a diatomic gas  $\nabla_{\text{ad}} = 2/7$ . We further explore how the atmosphere evolution varies with adiabatic index and molecular weight. We generate model atmospheres for monatomic adiabatic index  $\nabla_{\text{ad}} = 2/5$  and for a purely molecular hydrogen composition ( $\mu = 2$ ). The comparison between different gas compositions is deferred to section 5.3.

Figure 1 shows instantaneous atmosphere radial profiles at  $a = 10$  AU accreting around a fixed core of mass  $M_c = 5M_\oplus$  for several total planet masses. In what follows, if the  $R_B < R_H$  hierarchy holds, we define the planet mass as the total mass enclosed within the Bondi radius of the atmosphere, and regard the gas between the Bondi and Hill radii as perturbations due to the gravitational influence of the planet. For illustrative purposes we mark the position of the Bondi radius and of the radiative convective boundary. We notice that the pressure and temperature in the convective regions of the atmospheres scale as  $1/r$ , which is the expected behavior of an ideal gas adiabat with a polytropic equation of state (e.g., Rafikov 2006). In the outer radiative region of the atmosphere, the pressure has a nearly exponential profile, which is in agreement with the predictions of the analytic model (see section 3 and Appendix B). In addition, the atmosphere temperature at the radiative-convective boundary  $T_{\text{RCB}}$  only differs from the disk temperature  $T_d$  by an order unity factor, and so the atmosphere is nearly isothermal throughout the radiative zone. This is also in agreement with the analytic predictions.

The location of the Bondi radius moves further out as the mass of the atmosphere increases, as the Bondi radius scales with mass. The location of the radiative-convective boundary has a more interesting behavior. As stated in section 1, the nebular gas initially settles into equilibrium around the protoplanetary core on a short timescale relative to the thermal timescale, and is isen-

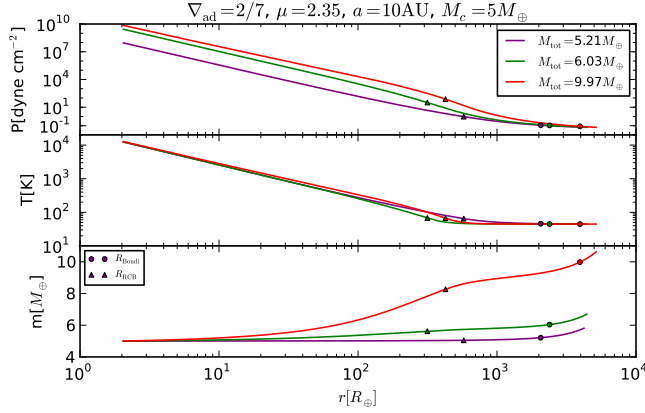


FIG. 1.— Example pressure, temperature and mass profiles as a function of radius.

tropic throughout with an entropy equal to that of the disk. In the context of our model, this atmosphere represents the minimum atmosphere mass for which a hydrostatic solution exists. This atmosphere is purely convective. As gas accumulates and the atmosphere starts cooling, an outer radiative region forms. This layer is thin for low mass atmospheres, as can be seen in Fig. 1: for the  $5.21M_{\oplus}$  atmosphere, the ratio between the thickness of the radiative and convective regions is low. An increase in atmosphere mass causes the radiative zone to expand and the convective region to contract. As more and more gas is accumulated, the convective zone eventually starts expanding again; however, the ratio between the radii of the radiative and convective regions continually increases with atmosphere mass, i.e. the radiative regions of these types of atmospheres are getting deeper and deeper. **[This needs to be rephrased, somewhat vague and repetitive.]**

We further use the global cooling model developed in section 2.4 to obtain an evolutionary series from static atmosphere profiles. Figure 2 shows the luminosity and cooling time evolution with atmosphere mass. Gas accretion is initially rapid, but slows down significantly after a relatively small mass increase. For comparison, we also plot the analytic results derived in section 3. We see that there is only a very brief agreement between the analytic and full numerical results. At early times, the radiative zone is too shallow and so the approximation that  $P_{RCB} \gg P_d$  used in section 3 breaks down. At late times, the self-gravity of the atmosphere becomes important.

#### 4.1. The End of Quasi-Static Evolution

The right-hand side of equation (22) decreases with increasing atmosphere mass, and eventually becomes negative when the mass of the envelope becomes comparable to the core mass  $M_{\text{atm}} \sim M_c$ . This implies a negative luminosity from the RCB. Physically, the luminosity  $L$  represents the total heat flux through the surface defined by the RCB. The heat flux due to convective motions is always directed outwards, and hence it is positive. Moreover, the temperature gradient  $dT/dr$  is negative, as the temperature decreases towards the outside. As a result (see equation (8d)), the heat flux due to radiative diffusion is also positive. This implies that, in the absence of

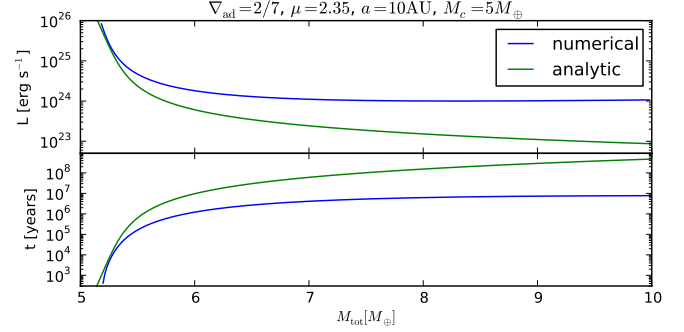


FIG. 2.— Luminosity and time evolution with mass. The analytic result is plotted for comparison.

planetesimal accretion and internal heat sources, there is no physical mechanism that can justify a negative luminosity. The quasi-static, constant luminosity approximation breaks down at this point and a more detailed, time-dependent model is necessary.

### 5. CRITICAL CORE MASS (PAPER I, EXCEPT FOR $\nabla_{\text{ad}} = 2/5$ CASE)

Standard static calculations of atmosphere accretion that consider planetesimal accretion as the main source of luminosity (e.g., Mizuno et al. 1978, Stevenson 1982, Rafikov 2006) find that an atmosphere can be stable only if the atmosphere mass is lower than the core mass. As the mass of the envelope becomes comparable to the solid core mass, the pressure gradient can no longer balance the self-gravity of the atmosphere, and hydrostatic equilibrium breaks down. As a result, a phase of rapid gas accumulation is initiated, i.e. runaway accretion. Typically, this instability settles in when  $M_{\text{atm}} \sim M_c$ . Static calculations do not take into account the time evolution of the atmosphere explicitly, but rather assume a steady state at which the luminosity due to planetesimal accretion is fully radiated away by the atmosphere. Therefore, for a set of disk and gas conditions, a single value for the critical core mass  $M_{\text{crit}}$  is found. This is the maximum mass the core can have before unstable gas accretion commences.

In our evolutionary model the core mass is assumed to be fixed, so the above definition for the critical core mass is not applicable. Nevertheless, we adopt a similar approach in defining the atmosphere mass past which hydrostatic balance no longer holds. We denote this mass as the minimum between the mass at which  $M_{\text{atm}} = M_c$  and the mass at which the right-hand side of equation (22) becomes negative (see section 4.1). We therefore define the evolutionary time (or growth time, or cooling time) of the atmosphere as the time elapsed until runaway accretion commences according to the criteria above. The evolution of atmosphere mass with time is shown in Figure 3 for  $a = 10$  AU and  $M_c = 5M_{\oplus}$ . Here,  $\Delta t$  is the instantaneous time step between subsequent static atmosphere models. We see that growth is slowest around  $M_{\text{tot}} \sim 6 - 7M_{\oplus}$ , after which it is continuously accelerated. The estimate of the atmosphere characteristic growth time is therefore insensitive to the exact choice of atmosphere mass to initiate runaway gas accretion, to order of magnitude, as long as it is past the time at which



accretion is slowest.

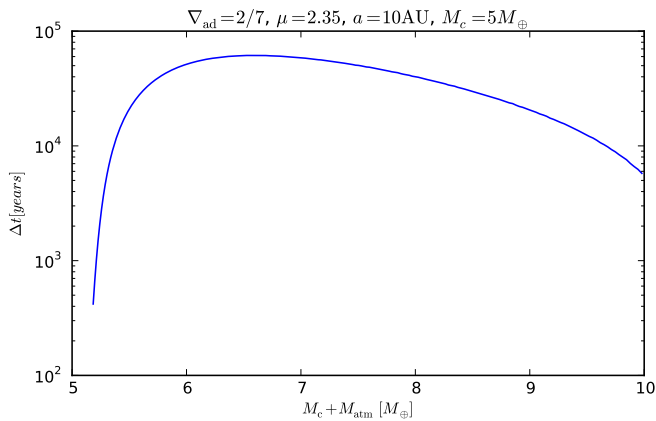


FIG. 3.— Instantaneous cooling time evolution with total mass. Accretion is slowest at  $M_{\text{tot}} \sim 6 - 7 M_{\oplus}$ .

### 5.1. Role of Disk Temperature and Pressure

In what follows we study the separate effect of disk temperature and pressure on the atmosphere growth time. At a fixed distance in the disk  $a = 10$  AU and for a core mass  $M_c = 5 M_{\oplus}$ , we fix the disk temperature  $T_d$  to the value given by equation (1b) and vary the disk pressure  $P_d$ . The resulting time evolution is plotted in Figure 4. We find that the atmosphere evolution time decreases as the disk pressure increases. This effect is likely due to the fact that a higher disk pressure, and hence density, leads to the atmosphere becoming self-gravitating and therefore initiating runaway accretion on a faster timescale. However, increasing the disk pressure by a factor of  $\sim 100$  only reduces the atmosphere growth time by a factor of  $\sim 2$ . As such, the atmosphere cooling time is only weakly dependent on the nebular pressure.

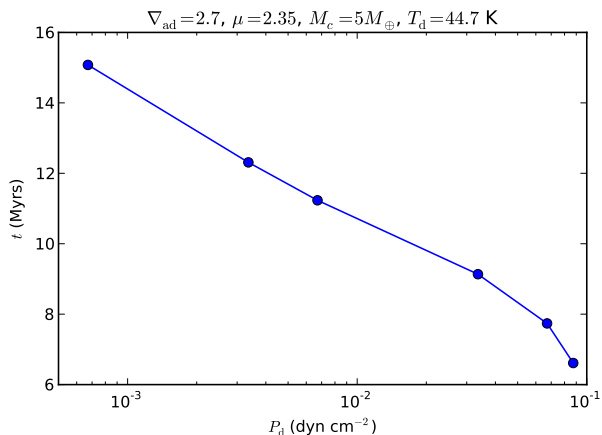


FIG. 4.— Disk pressure effect on growth time. Gas accretion is faster for higher pressures.

We perform a similar analysis on the effect of disk temperature  $T_d$  on the evolutionary time. For  $a = 10$  AU and  $M_c = 5 M_{\oplus}$ , we fix the disk pressure at the value given by equation (2) and vary  $T_d$ . The resulting dependence is shown in Figure 5. In contrast with the pressure

effect, an increase in disk temperature causes the growth time to increase as well. This is due to opacity effects: a higher disk temperature increases the opacity in the radiative zone of the atmosphere, causing a decrease in luminosity and therefore a longer Kelvin-Helmholtz accretion time. Moreover, a factor of  $\sim 3$  reduction in the disk temperature results in an decrease of the growth time by a factor of  $\sim 30$ . The atmosphere evolution is therefore strongly dependent on the temperature in the protoplanetary disk.

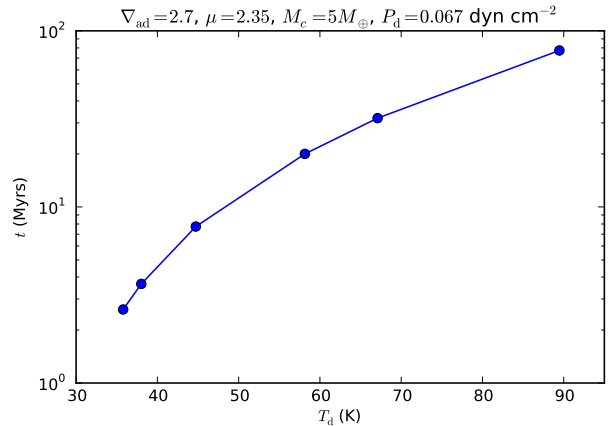


FIG. 5.— Disk temperature effect on growth time. Gas accretion is faster for lower temperatures.

### 5.2. Core Mass versus Evolution Time at Fixed Distance

In this section we explore how the core mass affects the cooling time of the atmosphere for a fixed semi-major axis. For consistency, we use the same distance as in the previous subsections  $a = 10$  AU. Figure 6 shows the growth time behavior for a range of cores with masses between 1 and 10  $M_{\oplus}$ . As expected, growth happens on a faster timescale if the core is more massive, as it can bind a gaseous atmosphere quicker due to its higher gravitational attraction. We find that the atmosphere growth time is very sensitive to the core mass: the core mass increase needed to reduce the cooling time by an order of magnitude is only half an Earth mass.

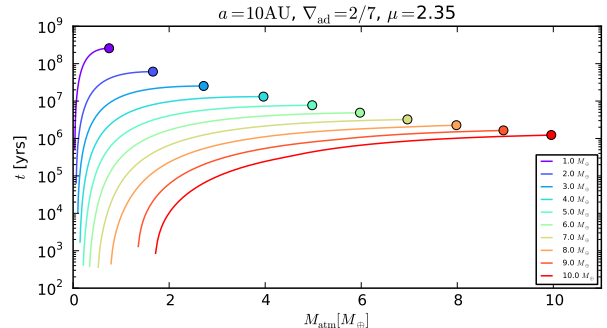


FIG. 6.— Time evolution as a function of atmosphere mass for a range of core masses. The circles mark the time when runaway accretion is initiated.

We further analyze how the thermodynamic properties

of the gas affect the atmosphere growth time. Specifically, we compare our standard model given by  $\nabla_{\text{ad}} = 2/7$  and  $\mu = 2.35$  with models with a different adiabatic index and mean molecular weight. This is shown in Figure 7. We discuss the effects of adiabatic index and molecular weight separately.

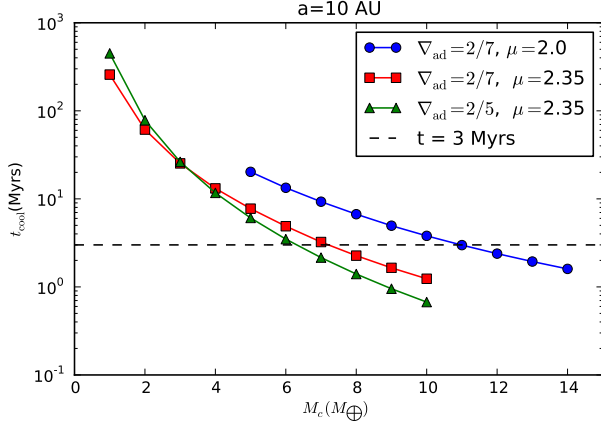


FIG. 7.— Time evolution for atmospheres with different adiabatic indices and mean molecular weight. A typical protoplanetary disk life time is plotted for comparison.

A decrease in the mean molecular weight of the gas results in a larger cooling time for the same core mass, since an atmosphere composed of heavier molecules is easier to bind. Moreover, a gas with a higher adiabatic gradient  $\nabla_{\text{ad}}$  is more dense, and therefore more likely to be bound by the gravity of the planet.

### 5.3. Critical Core Mass

In the previous subsections we explored and discussed the effect of various parameters on the growth time of an atmosphere accreting around a protoplanetary core of fixed mass. The main question we address right now is under what conditions can such an atmosphere grow before the gas in the protoplanetary disk is dissipated. Specifically, we determine the minimum core mass that is necessary for a protoplanet to initiate runaway gas accretion within the disk lifetime. We define this mass as the *critical core mass* for runaway growth.

Observations of protoplanetary disks show that they dissipate over a time scale of a few million years (e.g., Lagrange et al. 2000, Haisch et al. 2001, Goldreich et al. 2004). We adopt a disk life timescale of  $\tau = 3$  Myrs and determine the critical core mass as a function of gas and disk conditions. The results are displayed in Figure 8.

The critical core mass decreases as we move further away in the disk. This is due to several reasons:

- The disk temperature  $T_d$  is lower in the outer regions of the disk. As we showed in section 5.1, the atmosphere grows faster for lower temperatures, which offsets the need for a larger core mass.
- The gravitational attraction of the central star is weaker at larger distances, and hence the gravity of the protoplanet can act on a wider range.

Moreover, the critical core mass increases for a lower mean molecular weight and a smaller adiabatic gradient.

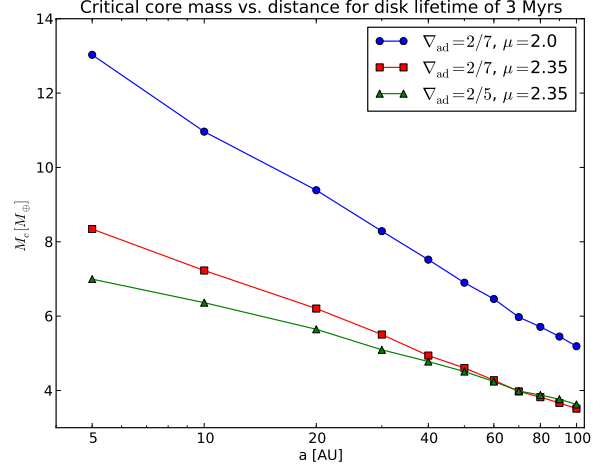


FIG. 8.— The minimum core mass for an atmosphere to become critical within the lifetime of the disk as a function of semi-major axis, for different adiabatic indices and molecular weight of the nebular gas.

This is consistent with the results derived in section 5.2. The critical core mass is strongly dependent on the mean molecular weight  $\mu$ , but only weakly dependent on the adiabatic index  $\gamma$  (or  $\nabla_{\text{ad}}$ ).

The comparison between our results and standard values for the critical core mass due to planetesimal accretion is deferred to section 6.1.

### 5.4. Opacity Dependence

In this section we investigate the effect of opacity reduction on the atmosphere evolution, since a lower opacity in the outer atmosphere regions accelerates gas accretion, resulting in a lower critical core mass. We explore opacity reductions by factors of 10 and 100, while keeping the power law (14) coefficient constant  $\beta = 2$ . The result is depicted in Figure 9.

We find that the atmosphere luminosity and growth time are increased and decreased, respectively, by factors of the same order as the opacity reductions.

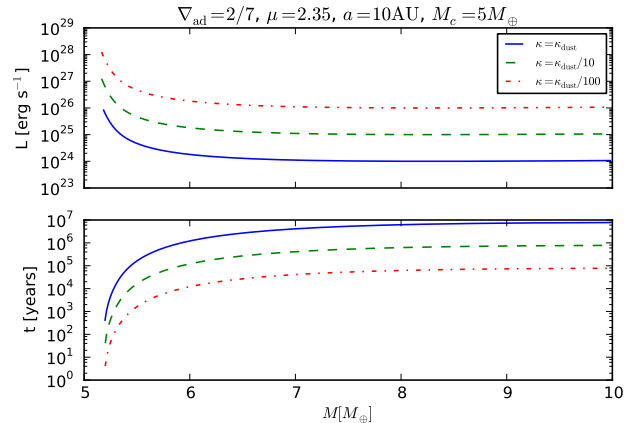


FIG. 9.— Comparison between standard dust opacity and opacity reduced by factor of 10 and 100, respectively. Lower opacity accelerates atmosphere growth.

## 6. DISCUSSION

In this section we discuss the parameter space of validity of our model. We calculate the conditions under which planetesimal accretion can be ignored, and review the effects of some of the approximations that come into our model.

### 6.1. Comparison with Planetesimal Accretion (*Paper II*)

In this study we have considered atmospheres for which planetesimal accretion is negligible and Kelvin-Helmholtz contraction dominates the luminosity evolution of the atmosphere. This is different from standard calculations, in which the atmosphere is heated by planetesimal accretion. In this section we investigate the core accretion rates that are necessary for our regime to be valid. We also discuss the conditions under which runaway gas accretion can be initiated due to the Kelvin-Helmholtz contraction of the atmosphere before it becomes critical due to planetesimal accretion.

We estimate the planetesimal accretion rate consistent with our assumptions that  $L_{\text{acc}} \ll L_{\text{KH}}$ . Here  $L_{\text{acc}}$  is the accretion luminosity given by

$$L_{\text{acc}} = G \frac{M_c \dot{M}_c}{R_c}, \quad (55)$$

where  $\dot{M}_c$  is the core accretion rate, and  $L_{\text{KH}}$  is the luminosity of the atmosphere due to gas contraction as calculated in section 4. At the limit,  $L_{\text{acc}} = L_{\text{KH}}$ . For a given atmosphere model we can therefore estimate the maximum planetesimal accretion rate during the gas contraction phase in order for the atmosphere to be dominated by the Kelvin-Helmholtz luminosity. We choose as a fiducial case an atmosphere forming at 10 AU and with a core mass of  $10M_\oplus$ . For this choice of parameters, the atmosphere cooling time is  $\sim 1.2$  Myrs (see Figure 7), which is within the typical life time of a protoplanetary disk. The results are presented in Figure 10.

We label the resulting minimum core accretion rate as  $\dot{M}_{c,\text{KH}}$ . The atmosphere growth rate is also plotted for comparison. We therefore see that the core accretion rate has to be  $\sim 2 - 3$  orders of magnitude lower than the atmosphere accretion rate for our assumptions to be valid. If the core had accreted planetesimals at this constant rate since it started forming, then the formation of a core massive enough to attract an atmosphere would not have been possible within typical disk life timescales, which indicates a slowing down of the planetesimal accretion regime. Possible explanations for that include the core having formed in the inner part of the disk and later migrated outwards, or the core having been depleted of planetesimals due to a giant neighbor. We also estimate the core accretion rate

$$\dot{M}_{c,\text{acc}}(M_c) \equiv \frac{M_c}{\tau} \quad (56)$$

needed for the core to form on the same timescale as our model atmosphere,  $\tau = 1.2$  Myrs, as well as a typical planetesimal accretion rate, for which the random velocities of the planetesimals are of the order of the Hill velocity around the protoplanetary core (Goldreich et al. 2004). We denote this latter rate as  $\dot{M}_{c,\text{typical}}$ . This rate,

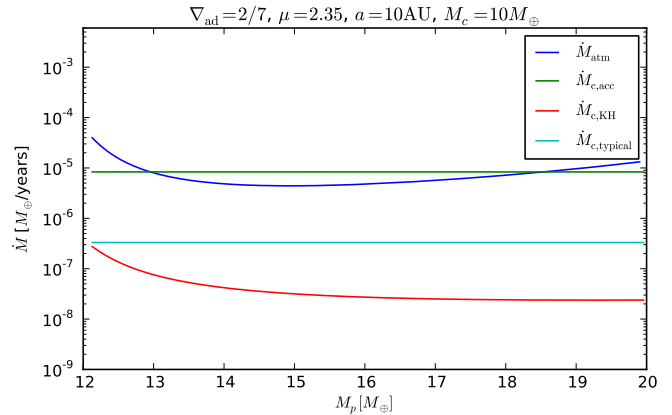


FIG. 10.— Various relevant accretion rates.  $\dot{M}_{\text{atm}}$  is the growth rate of the atmosphere as estimated by our model, and  $\dot{M}_{c,\text{KH}}$  is the maximum planetesimal accretion rate during the gas contraction phase in order for our regime to be valid. For comparison, we plot the core accretion rate  $\dot{M}_{c,\text{acc}}$  necessary to grow the core on the same time scale as the atmosphere  $\tau \sim 1.2$  Myrs, and a typical planetesimal accretion rate where the random velocity of the planetesimals is given by the Hill velocity due to the core.

which is at the boundary of the dispersion dominated and shear dominated regimes, is often quoted as a maximum (refs). However, it is easy to see that  $\dot{M}_{c,\text{typical}}$  is more than one order of magnitude lower than the gas accretion rate of our model atmosphere  $\dot{M}_{\text{atm}}$ , and lower than the core accretion rate  $\dot{M}_{c,\text{acc}}$  needed to grow the core and the atmosphere at the same time within the disk life time. As such, the formation of a giant planet by growing the core first, then letting the atmosphere cool is faster than growing the core and the atmosphere at the same time at a steady planetesimal accretion rate.

Next, we are interested in whether hydrodynamic gas accumulation due to planetesimal accretion can already commence before the atmosphere becomes unstable due to Kelvin-Helmholtz contraction, as our regime is no longer the relevant one under such conditions. A core that forms on the same timescale as our model atmosphere accretes planetesimals at a rate given by equation (56). This accretion rate is dependent on the core mass, which is steadily increasing. We therefore compare the critical core mass due to planetesimal accretion at this rate  $M_{\text{crit,acc}}$  to a core mass assumed fixed  $M_{c,\text{fixed}}$ . If  $M_{\text{crit,acc}} < M_{c,\text{fixed}}$ , then the atmosphere has already initiated unstable gas accretion by the time Kelvin-Helmholtz contraction starts dominating.

In order to estimate the critical core mass due to planetesimal accretion  $M_{\text{crit,acc}}$ , we use the results of Rafikov (2006) for low luminosity atmospheres forming in the outer disk ( $> 2 - 5$  AU), consistent with our region of interest. By relating his expression for the critical core mass to a given core mass dependent planetesimal accretion rate  $\dot{M}(M_c)$ , we find the following expression for the critical core mass when accretion luminosity dominates the evolution of the atmosphere:

$$M_{\text{crit,acc}} \sim \left[ \frac{\dot{M}(M_c)}{64\pi^2} \frac{\kappa_0}{\sigma G^3} \frac{1}{R_c M_c^{1/3}} \left( \frac{k}{\mu} \right)^4 \right]^{3/5}, \quad (57)$$

with all the constants as defined in previous sections. We therefore calculate  $M_{\text{crit,acc}}$  for a range of core masses. The result is displayed in Figure 11.

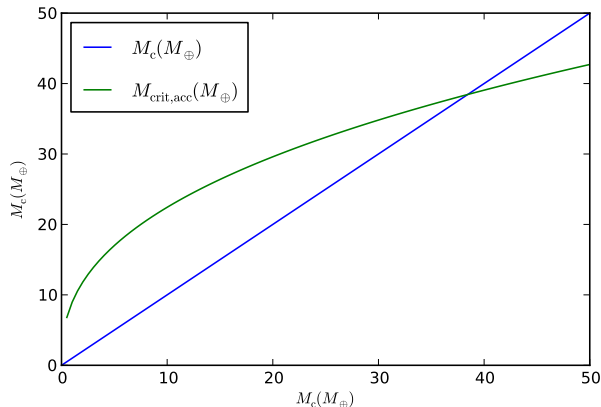


FIG. 11.— Comparison between the critical core mass  $M_{\text{crit,acc}}$  due to planetesimal accretion and the assumed fixed core mass when gas contraction dominates, for a growth time of  $\tau = 1.2$  Myrs. Unstable atmosphere collapse occurs due to core accretion before Kelvin-Helmholtz contraction starts dominating for core masses larger than  $\sim 40M_{\oplus}$ .

We see that the critical core mass due to planetesimal accretion is smaller than the mass of the fixed core for  $M_c \sim 40M_{\oplus}$ . This means that for large core masses, planetesimal accretion will lead to runaway gas accretion before gas contraction starts dominating, and hence our model is not applicable in that regime. However, we have found in section 5.3 that unstable atmospheres collapse occurs within the life time of the disk for protoplanetary cores smaller than this. We therefore confirm that planetesimal accretion can be safely ignored in our regime of interest. Moreover, as displayed in Fig. 10, it is faster to form a planet by growing the core first, then accreting a massive envelope, rather than by growing the core and atmosphere in parallel. **This works for this particular choice of core, disk etc. conditions, and I am expecting it to work for most of our parameter space, but it would probably be good to explore this numerically, at least to order of magnitude, with the estimates we have.**

As a final check, we investigate whether planetesimal accretion during the gas contraction phase at the rate  $\dot{M}_{\text{KH}}$  imposed by the condition that  $L_{\text{acc}} < L_{\text{KH}}$  can alter the core mass enough to affect the time evolution of the atmosphere. We can quantitatively estimate the increase in core mass as

$$\Delta M_c = \int_0^{t_{\text{crit}}} \dot{M}_c dt \approx \sum_i \dot{M}_{c,i} \Delta t_i, \quad (58)$$

where  $t_{\text{crit}}$  is the time elapsed until runaway gas accretion commences, and the accretion rate  $\dot{M}_{c,i}$  is given by

$$\dot{M}_{c,i} = \frac{L_i R_c}{GM_c} \quad (59)$$

from equation (55), with  $L_i$  the luminosity of the atmosphere at time  $t_i$  in our model. For  $M_c = 10M_{\oplus}$ ,

we find  $\Delta M_c \approx 0.05M_{\oplus}$ . This mass increase is therefore negligible in comparison with the initial core mass. It follows that a significant increase in core mass that could potentially alter the time evolution of the atmosphere would occur on a longer time scale than the mass-doubling time for the unperturbed atmosphere. Therefore, the time evolution of the atmosphere is insensitive to core mass changes at a rate imposed by the assumption that  $L_{\text{acc}} < L_{\text{KH}}$ .

## 6.2. Neglected Effects

In this section we summarize some of the simplifications we have made, and discuss their relative effect on our model.

### 6.2.1. Equation of State (Paper II)

In our model we assume an ideal gas law and a polytropic equations of state (EOS), given by equations (13) and (12), respectively. However, non-ideal effects such as partial dissociation and ionization have to be taken into account. One solution is using tabulated equation of state tables for hydrogen and helium mixtures. As future work, we plan to use the Saumon et al. (1995) EOS tables and extend them to lower pressures and temperatures as required by our disk assumptions.

### 6.2.2. Time Evolution (Paper I)

In this study we have assumed that the luminosity stays constant throughout the radiative region of the atmosphere. As a result, the time dependence can be neglected in equation (8d) and static solution can be obtained and then connected through a global cooling equations, as described in section 2.4. However, the assumption of constant luminosity breaks down for high atmosphere masses, as described in section 4.1; in this case, a time-dependent model is required to describe the atmosphere evolution. We are currently developing a full evolutionary time-dependent atmosphere model. We do not expect qualitatively different results. We showed in section 4.1 that the quasi-static model breaks down around the time when the atmosphere mass becomes equal to the mass of the core. Nevertheless, we can see from Figures 2 and 3 that the time of slowest accretion is safely before the region in which our model breaks down, and that the time after which the atmosphere mass increases by 25 % is only a factor of 2 lower than the mass doubling time. As a result, we are confident of our results to order of magnitude.

### 6.2.3. Inefficient Convection (Paper I)

#### Discussion about mixing length theory...

### 6.2.4. Opacity (Paper II)

In progress, still need to run models for smaller AU and see at what point ice grain opacity is no longer valid. Currently strange behavior at 1 AU for  $\nabla_{\text{ad}} = 2/5$ , the critical core mass goes up significantly instead of having a linear trend.  $\nabla_{\text{ad}} = 2/7$  atmospheres do not show this effect. Models for the inner disk would also show / confirm that close-in giant planet formation is hard (need larger core mass).

## 7. CONCLUSIONS

In this paper we have studied the formation of giant planet atmospheres under the assumption that Kelvin-Helmholtz gas contraction dominates the luminosity evolution of the atmosphere over planetesimal accretion. We built quasi-static two-layer atmosphere models with an inner convective region and an outer radiative region that matches smoothly onto the protoplanetary disk. We derived a cooling model to connect series of quasi-static atmospheres, and thus obtained an evolutionary history of the envelope. We defined the time at which unstable atmosphere collapse commences as  $M_{\text{atm}}(t) \sim M_c$ . From this we defined as “critical core mass” the minimum core mass for a protoplanet to initiate runaway gas accretion during the lifetime of the protoplanetary disk. We studied this minimum mass for a variety of disk conditions, nebular gas compositions and opacities. We found that

the critical core mass decreases as we move further out in the disk, and is smaller for lower disk temperatures and opacities and for higher mean molecular weight of the gas.

We find that the critical core mass to form a giant planet within the life time of the disk is smaller than the results yielded by studies that assume that the atmosphere evolution is dominated by the luminosity due to planetesimal accretion. We have showed that the planetesimal accretion rate needed to grow the core on a typical disk time scale is larger than the expected planetesimal accretion rates at large separations. As such, it is faster to form a planet by growing the core first in a fast planetesimal accretion regime (e.g., the core forms in the inner disk, then migrates outwards), then significantly reduce planetesimal accretion and allow a massive atmosphere to accumulate.

## REFERENCES

- Bell, K. R. & Lin, D. N. C. 1994, *ApJ*, 427, 987  
 Chiang, E. & Youdin, A. N. 2010, *Annual Review of Earth and Planetary Sciences*, 38, 493  
 D’Angelo, G., Durisen, R. H., & Lissauer, J. J. *Giant Planet Formation*, ed. S. Piper, 319–346  
 Goldreich, P., Lithwick, Y., & Sari, R. 2004, *ARA&A*, 42, 549  
 Haisch, Jr., K. E., Lada, E. A., & Lada, C. J. 2001, *ApJ*, 553, L153  
 Ikoma, M., Nakazawa, K., & Emori, H. 2000, *ApJ*, 537, 1013  
 Kippenhahn, R. & Weigert, A. 1990, *Stellar Structure and Evolution*  
 Lagrange, A.-M., Backman, D. E., & Artymowicz, P. 2000, *Protostars and Planets IV*, 639  
 Mizuno, H., Nakazawa, K., & Hayashi, C. 1978, *Progress of Theoretical Physics*, 60, 699  
 Papaloizou, J. C. B. & Nelson, R. P. 2005, *A&A*, 433, 247  
 Papaloizou, J. C. B. & Terquem, C. 1999, *ApJ*, 521, 823  
 Rafikov, R. R. 2005, *ApJ*, 621, L69  
 —. 2006, *ApJ*, 648, 666  
 Saumon, D., Chabrier, G., & van Horn, H. M. 1995, *ApJS*, 99, 713  
 Semenov, D., Henning, T., Helling, C., Ilgner, M., & Sedlmayr, E. 2003, *A&A*, 410, 611  
 Stevenson, D. J. 1982, *Planet. Space Sci.*, 30, 755  
 Thompson, M. J. 2006, *An introduction to astrophysical fluid dynamics*  
 Wuchterl, G. 1993, , 106, 323

## APPENDIX

### DERIVATION OF GLOBAL ENERGY EQUATION

We derive here the global energy equation (16). We follow the simpler example in §4.3 of Kippenhahn & Weigert (1990), adding the effects of finite core radius, surface pressure and mass accretion. We assume that hydrostatic balance holds. Integrating the local energy equation (19) from core to surface gives:

$$L - L_c = \int_{M_c}^M \frac{\partial L}{\partial m} dm \quad (\text{A1a})$$

$$= \int_{M_c}^M \left( \epsilon - T \frac{\partial S}{\partial t} \right) dm \quad (\text{A1b})$$

$$= \Gamma - \int_{M_c}^M \frac{\partial u}{\partial t} dm + \int_{M_c}^M \frac{P}{\rho^2} \frac{\partial \rho}{\partial t} dm. \quad (\text{A1c})$$

with  $\Gamma = \int \epsilon dm$  the integral of the direct heating rate.

In what follows, we must carefully distinguish between partial time derivatives,  $\partial/\partial t$ , (performed at fixed mass) and total time derivatives, denoted with overdots (which include the effect of mass accreted through the outer boundary). For instance the surface radius,  $R$ , evolves as

$$\dot{R} = \frac{\partial R}{\partial t} + \frac{\dot{M}}{4\pi R^2 \rho_M} \quad (\text{A2})$$

where  $\partial R/\partial t$  gives the Lagrangian contraction of surface mass elements, and  $\dot{M}$  denotes mass accretion rate through the upper boundary. The subscript  $M$  denotes quantities at the upper boundary of total mass  $M$  (though it is omitted

from  $M$  and  $R$ ). Similarly the volume,  $V = (4\pi/3)r^3$  and pressure at the surface evolve as

$$\dot{V}_M = \frac{\partial V_M}{\partial t} + \frac{\dot{M}}{\rho_M} \quad (\text{A3a})$$

$$\dot{P}_M = \frac{\partial P_M}{\partial t} + \frac{\partial P_M}{\partial m} \dot{M} \quad (\text{A3b})$$

$$= \frac{\partial P_M}{\partial t} - \frac{GM}{4\pi R^4} \dot{M}. \quad (\text{A3c})$$

For the purpose of this derivation we will hold the core mass fixed  $\dot{M}_c = 0$  which further gives  $\dot{P}_c = \partial P_c / \partial t$ .

To derive the global energy equation we must move the (partial) time derivatives in Equation (A1c) outside their integrals. The internal energy integral follows simply from Leibniz's rule as

$$\int_{M_c}^{M(t)} \frac{\partial u}{\partial t} dm = \dot{E}_i - \dot{M} u_M. \quad (\text{A4})$$

To evaluate the work integral, we derive a pair of expressions for the rate of change of gravitational energy. The time derivative of Equation (20) gives

$$\begin{aligned} \dot{E}_G = & 3 \int_{M_c}^M \frac{P}{\rho^2} \frac{\partial \rho}{\partial t} dm - 3 \int_{M_c}^M \frac{\partial P}{\partial t} \frac{dm}{\rho} \\ & - 3 \frac{P_M}{\rho_M} \dot{M} + 3 \dot{P}_M V_M - 3 \dot{P}_c V_c + 3 P_M \dot{V}_M. \end{aligned} \quad (\text{A5})$$

The first integral in Equation (A5) is the one we want, but the next one must be eliminated. The time derivative of Equation (17) (times four) gives

$$4\dot{E}_G = -4 \frac{GM\dot{M}}{R} + 4 \int_{M_c}^M \frac{Gm}{r^2} \frac{\partial r}{\partial t} dm \quad (\text{A6a})$$

$$= -4 \frac{GM\dot{M}}{R} + 4\pi \int_{M_c}^M r^3 \frac{\partial}{\partial m} \frac{\partial P}{\partial t} dm \quad (\text{A6b})$$

$$\begin{aligned} &= -4 \frac{GM\dot{M}}{R} - 3 \int_{M_c}^M \frac{\partial P}{\partial t} \frac{dm}{\rho} \\ &\quad + 3 V_M \frac{\partial P_M}{\partial t} - 3 V_c \frac{\partial P_c}{\partial t} \end{aligned} \quad (\text{A6c})$$

where Equations (A6b) and (A6c) use hydrostatic balance and integration by parts.

Subtracting Equations (A4) and (A6c) and rearranging for the desired integral gives

$$\int_{M_c}^M \frac{P}{\rho^2} \frac{\partial \rho}{\partial t} dm = -\dot{E}_G - \frac{GM\dot{M}}{R} - P_M \frac{\partial \dot{V}_M}{\partial t} \quad (\text{A7})$$

with Equation (A3) used to combine terms. Combining Equations (A1c), (A4) and (A7), we reproduce Equation (16) with the accreted energy  $e_{\text{acc}} \equiv u_M - GM/R$ .

## ANALYTIC COOLING MODEL DETAILS

### *Estimate of Atmosphere Mass Outside the Bondi Radius*

Here we consider the mass exterior to the Bondi radius. For a meaningful evaluation we only include the mass coming from the overdensity relative to the background density. The resulting external mass for an isothermal atmosphere is

$$M_{\text{ext}} = 4\pi \int_{R_B}^{r_{\text{fit}}} (\rho - \rho_o) r^2 dr \quad (\text{B1a})$$

$$\begin{aligned} &= M_c \theta_c \int_1^{n_{\text{fit}}} 3 \left[ \exp \left( \frac{1}{x} - \frac{1}{n_{\text{fit}}} \right) - 1 \right] x^2 dx \\ &\equiv M_c \theta_c I(n_{\text{fit}}) \end{aligned} \quad (\text{B1b})$$

where  $\theta_c = R_B/R_c$  and the dimensionless integral  $I(n_{\text{fit}})$  obeys the limits  $I(1) = 0$  and  $I \rightarrow n_{\text{fit}}^2/2$  as  $n_{\text{fit}} \rightarrow \infty$ . Since this external mass does not converge, the choice of an outer boundary does matter in principle. In practice, however,

the assumption that  $r_{\text{fit}} = R_{\text{H}}$  limits  $n_{\text{fit}}$  to modest values

$$n_{\text{fit}} = \frac{R_{\text{H}}}{R_{\text{B}}} \approx 1.3 \frac{a_{10\oplus}^{4/7}}{m_{c10\oplus}^{2/3} m_*^{1/3}}. \quad (\text{B2})$$

Since for instance  $I(2) = 1.1$ , these modest  $n_{\text{fit}}$  values will only produce a small external mass.

#### The Opacity Effect

A lower opacity could lower the core mass. Reducing the opacity by a factor of one hundred cuts the core mass by more than a factor of 10, specifically to  $9 M_{\oplus}$  for the parameters in Equation (54). The reduction is not as strong as the nominal scaling would imply,  $0.01^{3/5} \approx 0.06$ , because  $\xi$  increases.

Even with significantly lower opacities, radiative diffusion remains a good approximation at the radiative-convective boundary. We estimate the optical depth as (for  $\beta = 2$ ):

$$\tau_{\text{RCB}} \sim \frac{\kappa P_{\text{RCB}}}{g} \sim 7 \times 10^4 \frac{F_T^4 F_{\kappa}}{\left(\frac{m_{c\oplus}}{10}\right) \left(\frac{a_{\oplus}}{10}\right)^{\frac{12}{7}}} \quad (\text{B3})$$

where  $P_{\text{RCB}} \sim P_M$  for a self-gravitating atmosphere and  $g \sim GM_c/R_B^2$ , with both approximation good to within the order unity factor  $\xi$ . Clearly  $\tau_{\text{RCB}} \gg 1$  even for  $F_{\kappa} \lesssim 0.01$  out to very wide separations.

A hotter disk would increase core masses. Instead of our passive disk model, adopting the standard Hayashi temperature profile would increase core masses by  $\sim 50\%$ . A hotter accretion phase would further increase core masses, but such phases are presumably short lived.

#### Surface Terms

We now check the relevance of the neglected surface terms in Equation (16). We already showed that accretion energy can be exactly eliminated by choosing an outer boundary near the Bondi radius. We now show that accretion energy is also a small correction at the RCB. A rough comparison, (ignoring terms of order  $\xi$ ) of accretion luminosity vs.  $\dot{E}$  gives

$$\frac{GM\dot{M}}{R\dot{E}} = \frac{GM}{R} \frac{dM}{dE} \sim \frac{GM_c^2}{R_B E} \frac{P_{\text{RCB}}}{P_M} \sim \sqrt{\frac{R_c}{R_B}} \ll 1, \quad (\text{B4})$$

where we assume  $P_{\text{RCB}} \sim P_M$  for a massive atmosphere. Accretion energy at the protoplanetary surface is thus very weak for marginally self-gravitating atmospheres, and even weaker for lower mass atmospheres. A similar scaling analysis shows that the work term,  $P_M \partial \dot{V}_M / \partial t$  is similarly weak. Nevertheless our numerical calculations include these surface terms in a more realistic and complete model of self-gravitating atmospheres.

#### Hydrogen Dissociation

The dissociation of molecular hydrogen deep in the atmospheres of accreting protoplanets plays a significant role in the energetics of core accretion. In the high density regions  $r \ll R_{\text{RCB}}$  of a convective atmosphere, the thermal plus gravitational energy scales as

$$dE = -4\pi \nabla_{\text{ad}}^{1/\nabla_{\text{ad}}} \rho_{\text{RCB}} R_B^{1/(\gamma-1)} r^{\frac{2\gamma-3}{\gamma-1}} \frac{dr}{r} \quad (\text{B5})$$

If  $\gamma < 3/2$  then the main contribution to the energy is at the bottom of the atmosphere, i.e. the core. This is the case for a diatomic ideal gas ( $\gamma = 1.4$ ) or a solar mixture of hydrogen and helium ( $\gamma \approx 1.43$ ). However a monatomic gas has  $\gamma = 5/3 > 3/2$ . In this case, the atmosphere's energy is no longer concentrated near the bottom, but will be concentrated near the top of the convective zone.

A likely structure is an atmosphere that is dissociated near the base, but becomes molecular near the top of the convective zone. In this case the atmosphere's energy budget would be concentrated near the atomic to molecular transition.

The energy required to dissociate a hydrogen molecule,  $I = 4.467$  eV can be significant to the overall energy budget. Since

$$\frac{I}{\nabla_{\text{ad}} GM_c (2m_{\text{H}})/r} \approx 3 \left( \frac{M_c}{10M_{\oplus}} \right)^{-2/3} \frac{r}{R_c} \quad (\text{B6})$$

we see that this energy is always relevant.

We can use the Saha equation to determine where dissociation is significant,

$$\frac{n_{\text{H}}^2}{n_{\text{H}_2}} = \left( \frac{\pi m_{\text{H}} k T}{h} \right)^{3/2} e^{-I/(kT)} \quad (\text{B7})$$

We introduce a reaction coordinate  $\delta$  so that  $n_{\text{H}} = 2\delta n_o$  and  $n_{\text{H}_2} = (1-\delta)n_o$  with  $n_o = \rho X/(2m_{\text{H}})$  the number density when all hydrogen is molecular. We express equilibrium as

$$\frac{\delta^2}{1-\delta} = f_{\mu} \frac{P_{\text{diss}}(T)}{P} \quad (\text{B8})$$

TABLE 1  
PARAMETERS DESCRIBING STRUCTURE OF RADIATIVE ZONE.

$\gamma = 7/5$ ( $\nabla_{\text{ad}} = 2/7$ ), $\alpha = 0$					
$\beta$	1/2	3/4	1	3/2	2
$\nabla_{\infty}$	2/7 <sup>a</sup>	4/13	1/3	2/5	1/2
$\chi$	...	2.25245	1.91293	1.65054	1.52753
$\theta$	...	0.145032	0.285824	0.456333	0.556069

<sup>a</sup> Since  $\nabla_{\text{ad}} = \nabla_{\infty}$  there is no convective transition at depth for this case.

with the characteristic pressure below which dissociation occurs is

$$P_{\text{diss}} = \frac{(kT)^{5/2}}{4} \left( \frac{\pi m_{\text{H}}}{h^2} \right)^{3/2} e^{-I/(kT)} \quad (\text{B9})$$

and the order unity factor

$$f_{\mu} = 2\delta + (1 - \delta) + Y/2 + Z/\mu_Z \quad (\text{B10})$$

accounts for variations in the mean molecular weight with dissociation. (Take  $\mu_Z = 31/2$ , but not too significant.)

Thus dissociation occurs where  $P \lesssim P_{\text{diss}}(T)$ . At disk temperatures (say 150 K) the dissociation pressure is negligibly small ( $\sim 10^{-141}$  dyne cm<sup>-2</sup>) and no dissociation occurs. However at core temperatures the dissociation pressure is quite large especially for massive cores. Dissociation is guaranteed.